Accepted on 5 October 2005
JZS doi: 10.1111/j.1439-0469.2005.00349.x

CONICET – Instituto de Bio y Geociencias y Museo de Ciencias Naturales, Universidad Nacional de Salta, Mendoza 2, 4400-Salta, República Argentina

Morphological evolution of Ceratophryinae (Anura, Neobatrachia)

M. Fabrezi

Abstract

Body form is one of the major consequences of development, and diversification of body shapes implies developmental changes among species. In anurans, changes in the timing of developmental events or heterochrony, have been emphasized as a source of variation in the patterns of development that has lead to diverse morphology. Herein, different approaches are used to explore morphological traits in members of the Ceratophryinae (Anura: Leptodactylidae), a group of frogs with some features produced by overdevelopment. Cladistic analyses were conducted in order to distinguish the shared history of *Ceratophrys, Chacophrys* and *Lepidobatrachus* and other anurans. From these studies, morphological variation of selected skeletal features in ceratophryines reveals the presence of ancient structures, which have been considered lost in the neobatrachian phylogeny, integrated in particular designs. Thin-plate spline morphometric analyses of skull shapes among ceratophryines describe *Lepidobatrachus* as the most distinctive shape. Moreover, thin-plate spline morphometric analyses among anurans show divergent skull shapes between ceratophryines and other anurans, reflecting that the skull shapes of ceratophryines are a result of peramorphosis (increase of developmental rates). This study represents the first detailed examination of the role of peramorphosis in a clade of anurans.

Key words: Anura – ontogeny – heterochrony – variation – Ceratophryinae

Introduction

South American frogs of genera *Ceratophrys*, *Chacophrys*, *Lepidobatrachus*, *Macrogenioglottus*, *Odontophrynus*, and *Proceratophrys* are included in Ceratophryinae (Frost 2004), which is placed within the paraphyletic Leptodactylidae (Ford and Cannatella 1993). Laurent (1986) divided the subfamily into two tribes: Ceratophrynini, with *Ceratophrys*, *Chacophrys*, and *Lepidobatrachus*; and Odontophrynini with *Macrogenioglottus*, *Odontophrynus*, and *Proceratophrys*. Other authors did not follow this criterion and Duellman (1993) restricted the subfamily to include only Laurent's tribe Ceratophrynini. This study focuses on morphological characteristics among the three former genera and uses the taxon name Ceratophryinae following Frost (2004).

Monophyly of *Ceratophrys*, *Chacophrys*, and *Lepidobatrachus* was recognized by immunology (Maxson and Ruibal 1988) and morphology (Reig and Limeses 1963; Lynch 1971; Cei 1981; Wassersug and Heyer 1988; Hanken 1993; Haas 2003; among others). Adults of these genera share a set of morphological features such as macrocephalia, megalophagia, and aggressive behavior (Hanken 1993). Many morphological traits are integrated in this distinctiveness. In contrast, tadpoles of the ceratophryines show noticeable intergeneric differences. Thus, the set of features of ceratophryines appears after metamorphosis.

In the literature describing shape variation among small and miniature frogs characterized by patterns of paedomorphosis, diversification is interpreted primarily as a result of an ecological shift from an aquatic to a terrestrial environment (Clarke 1996). This diversification involved fossoriality, tendency toward reduced body size, and suppression of larval development (Clarke 1996; Hanken et al. 1997). Most of these trends can explain diversification among anuran groups with small and miniature species (e.g. arthroleptids, petropedetids, and dendrobatids). Ceratophryines, however, are characterized by forms of medium to large body size, and they have both terrestrial and aquatic habits. Size and morphological variation appear to reflect opposing (or inverted) patterns of development to those previously described, and therefore may involve distinctive ecological and evolutionary consequences.

Although much is known about the morphology of the ceratophryines, there is little comparative information on morphological variation and how development could have played a role in shaping the Ceratophryinae body plan. The following account describes some selected traits of the skeleton and skull shapes of ceratophryines, emphasizing those features resulting from a peramorphic pattern of development in order to: (1) compare morphological variation among ceratophryines; (2) identify morphological traits that distinguish ceratophryines from other anuran taxa; and (3) discuss peramorphic development as an evolutionary process.

Materials and Methods

Data in this study are subjected to three different analyses: (1) cladistic analysis in order to address relationships of *Ceratophrys cranwelli*, *Chacophrys pierottii*, *Lepidobatrachus laevis*, *Lepidobatrachus llanensis*, and other anurans; (2) morphological descriptions of variation in selected osteological traits of ceratophryines; and (3) thin-plate spline morphometrics (TPS) analyses to describe skull shape and skull shape changes within ceratophryines and other anurans.

Morphological studies for all analyses were exclusively derived from this study. Species, specimen numbers, and collection data are listed in Appendix 1. Osteological whole-mounts were obtained following Wassersug (1976) and included larval, juvenile, and adult specimens of ceratophryines (Appendix 1). The normal table of Gosner (1960) was used for staging larvae. Observations and photographs were made using a stereo microscope.

For Cladistic analysis a total of 81 morphological characters were scored for 62 anuran species belonging to Bombinatoridae, Pipidae, Scaphiopodidae, and 12 neobatrachian families (see Appendix 1). *Bombina variegata* (Bombinatoridae) was chosen as outgroup. Characters used were obtained primarily from skeletons, and only a few characters correspond to larval morphology or general morphology (Appendix 2). All characters were analyzed as non-additive (Appendix 3). Phylogenetic analyses were done using parsimony software (TNT: Tree Analysis Using New Technology, vers. 1.0) by Goloboff et al. (2003). The data set was studied with two criteria: (a) equally weighted character analysis, and (b) implied weighting method

(Goloboff 1993) applying different values for constant concavity ($K = 1$, $K = 2$, and $K = 3$). Robustness of branches was evaluated performing jacknifing (Lanyon 1985).

Thin-plate spline morphometrics analyses were carried out to describe shape and shape changes in ceratophryines, and for comparison with other anurans. TPS methods allow the description of shape changes using a set of landmark data independent of size, location, and orientation (Bookstein 1991). Landmarks points for thin-plate spline analyses were selected following a previous study (Yeh 2002) and two analyses were performed: 'dorsal skull' and 'lower jaw', with 14 and 7 landmarks respectively as depicted in Fig. 1. Dorsal skull and lower jaw drawings of each specimen were obtained using an Olympus SZH microscope with attached camera lucida, scanned, and landmark points digitalized only on one side of the view to avoid asymmetry using TPSDig 1.4 (Rohlf 2004a). For each specimen, decomposition of shape into orthogonal 'principal warps' provides a set of principal-warp coefficients that describe its deviation from a generalized orthogonal least-square Procrustes consensus configuration. Relative-warps (RWs) analyses result from a principal-component analysis of the principal-warp coefficients and permit the description of the primary axes along which shape changes occurs (Bookstein 1991). RW analyses were conducted using TPSrelw 1.37 (Rohlf 2003) to study 'dorsal skull' and 'lower jaw' in (1) a sample of 17 specimens of *C. cranwelli*, *C. pierottii*, *L. laevis*, and *L. llanensis*, and (2) a sample of 50 anuran species representing 15 families (Appendix 1). Scatterplots of RW scores were examined to compare deformations among specimens and species respect of the consensus configuration. TPS-thin-plate spline 1.19 (Rohlf 2004b) allowed to visualize shape changes along RWs.

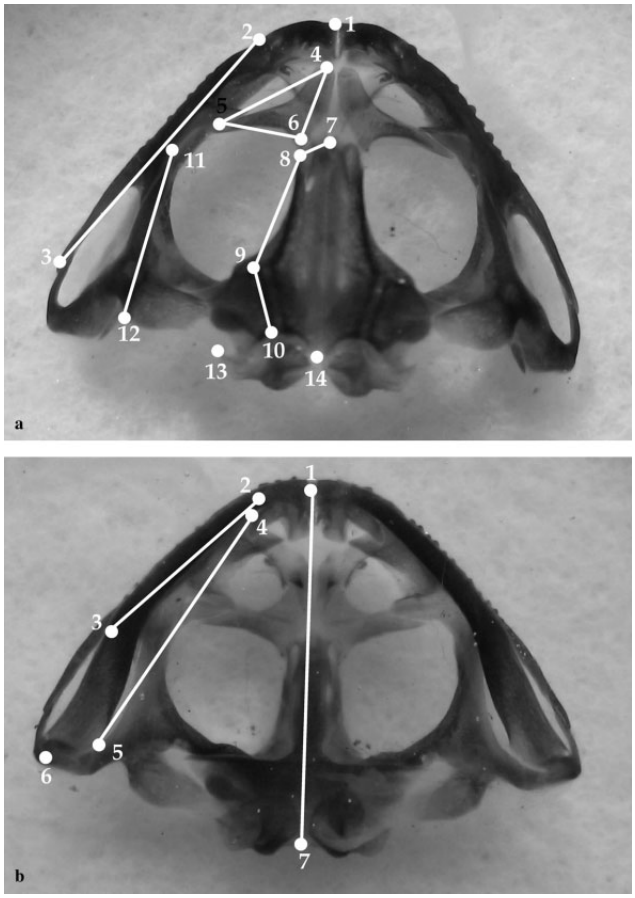

Fig. 1. Representation of selected landmarks used for thin-plate spline analyses. (a) Dorsal skull landmarks: 1, point between premaxillae; 2–3, anterior and posterior tips of maxillary; 4–5–6, tips of nasal; 7–8–9–10, more external points of frontoparietal; 11–12, anterior and posterior tips of squamosal; 13, posterior tip of otic capsule; 14, the most posterior middle point of skull. (b) Lower jaw landmarks; 1, mandibular symphysis; 2–3, anterior and posterior tips of dentary; 4–5, anterior and posterior tips of angulosplenial; 6, posterior end of lower jaw; 7, point between occipital condyles. All landmarks were digitalized on the left side of dorsal skull and right side of lower jaw

Results

Ceratophryinae relationships

Cladistic analyses with implied weighting method show high support for the monophyly of pipids, scaphiopodids and some neobatrachian taxa (Ceratophryinae, *Bufo* spp., *Leptodactylus* spp., *Phrynobatrachus* spp., *Ptychadena* spp., *Hoplobatrachus* plus Pyxicephalinae, and Arthroleptidae) (Jacknifing absolute values > 50 in Fig. 2). Ceratophryines, always monophyletic, appear as the sister taxon of all neobatrachians although in the strict consensus obtained with criterion of equally weighted characters, no relationships among pipids, pelobatids and neobatrachians can be proposed.

Heuristic searches with 1000 random-addition sequences replicates with the criterion of equally weighted characters found minimal-length topologies of 468 steps (CI 0.2711; RI 0.693). The branch swapping algorithm used was tree bisection and reconnection (TBR) and minimal-length trees replicates led to 2362 trees. Their strict consensus tree recovered Ceratophryinae's monophyly. For this analysis, the jacknifing value for ceratophryines is 99. Relationships within ceratophryines are less well supported; although the clade formed by *Lepidobatrachus* spp. reaches a jackknifing value of 89.

Using the implied weighting method, statistical coefficients of CI and RI exhibit light variation compared with the equally weighted characters method [$K = 1$ (CI = 0.25, RI = 0.666); $K = 2$ (CI = 0.256, RI = 0.669); and $K = 3$ (CI = 0.258, RI = 0.672)] and their results are more congruent to previous hypothesis (Ford and Cannatella 1993). All analyses found ceratophryines as a monophyletic group. Heuristic searches with 1000 random-addition sequences with implied weighting $K = 2$ led to three trees with 389 steps with a best score of 40.03388. The trees display differences in the position of some taxa (*Astylosternus diadematus*, *Scinax fuscovarius*) but most taxa do not vary. Relationships represented in tree 0 (Fig. 2) were considered enough to focus derived characters in the morphology of ceratophryines. Jacknifing support (with an independent character removal = 25) has values of 90 for ceratophryines, 68 for *Chacophrys* plus *Lepidobatrachus*, and 60 for *Lepidobatrachus* (Fig. 2). Monophyly of pipids, scaphiopodids, and neobatrachians are in agreement with current hypotheses on the phylogeny of frogs (Ford and Cannatella 1993), and unsolved relationships within suprageneric bufonoid and ranoid taxa are still the subject of discussion and study.

Synapomorphies defining the clade Ceratophryinae (Fig. 2) correspond to characters 2, 8, 11, 12, 14, 23, 24, 29, and 30; characters 23, 29, and 30 being autoapomorphies. Characters 2 (skull exostosis), 8 (presence of arch parieto-squamosal), 11 (zygomatic ramus of squamosal reaching the maxilla), and 12 (monocuspid teeth) are shared with some scaphiopodids, pipids, ranids, bufonids and hylids; this set of characters involves extensive development of skull bones. Character 14 (absence of pars palatina of premaxilla) occurs in some pipids and ceratophryines. Character 24 (strong fusion of dentary and mentomeckelian) appears in some ranids and ceratophryines. Character 23 (spur-like fang formed by dentary and mentomeckelian bones) is one of the autoapomorphies of the

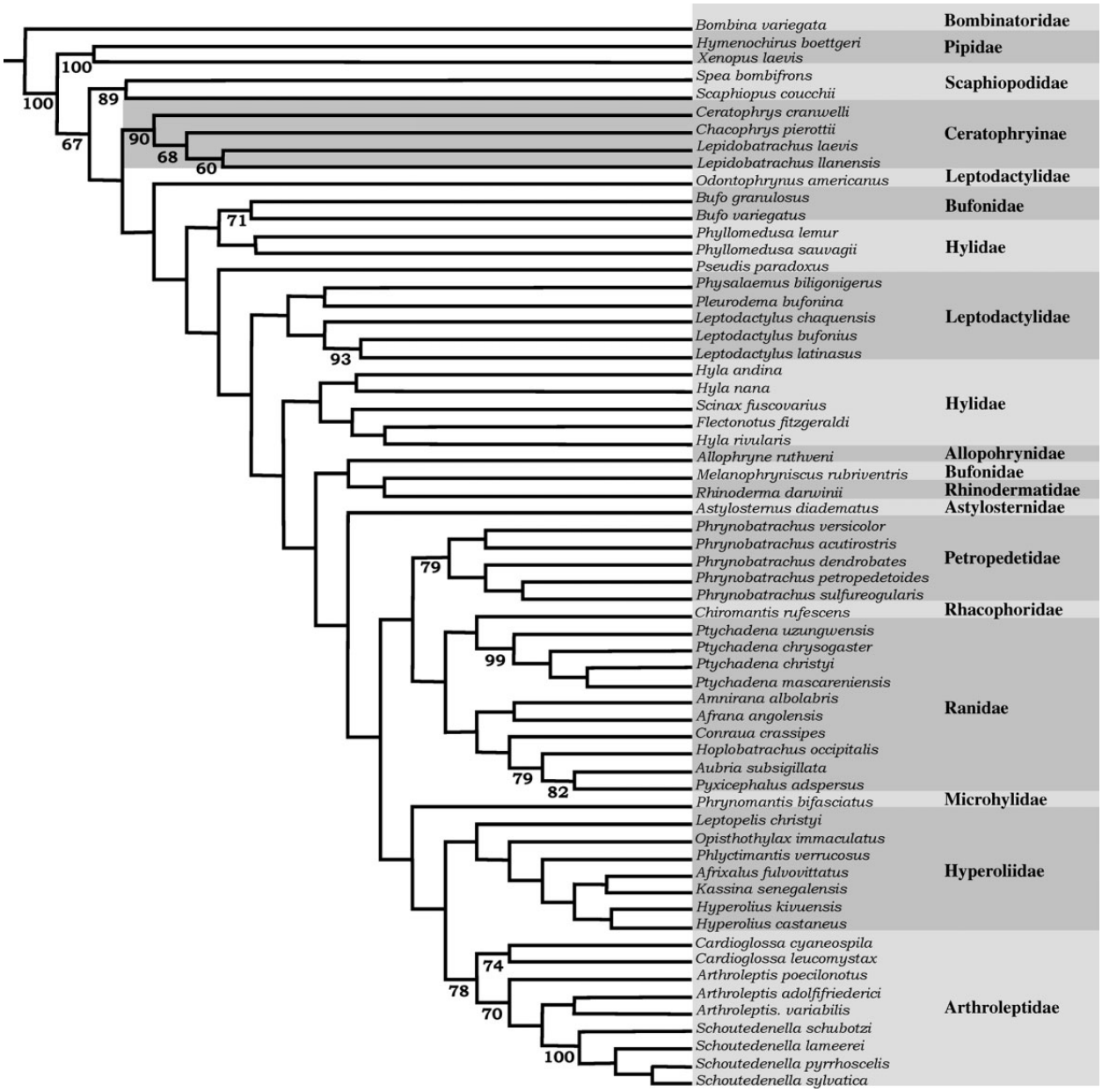

Fig. 2. Phylogenetic relationships among anuran species belonging to 16 suprageneric taxa. This tree was obtained by the implied weighting method ($K = 2$) in TNT (Goloboff et al. 2003). Numbers below branches show jacknifing absolute values (Lanyon 1985)

group. *Ceratophrys* is the sister group of *Chacophrys* plus *Lepidobatrachus*. Synapomorphies of *Ceratophrys* are characters 44 (dorsal shields, see Fig. 4b) and 45 (transverse processes of eighth presacral vertebra oriented forward). This last character exhibits 12 steps in the tree. The synapomorphy of the clade containing *Chacophrys* plus *Lepidobatrachus* (character 32) is the presence of a well developed parahyoid bone (Fig. 3c–f). Synapomorphies for the *Lepidobatrachus* node are represented by characters 25 (discontinuous ceratohyalia, Fig. 3d–f), also present in scaphiopodids; 75 (presence of double spiracles in tadpoles), as in pipid tadpoles; and 77 (absence of keratodonts), as in pipid and microhylid tadpoles. Synapomorphic characters of *Chacophrys* (52, presence of ileal ridge) and *L. laevis* (60 and 61; terminal phalanx of toe IV curved and pointed) appear many times (52, 9 steps; 60, 12 steps; and 61, 16 steps). *Lepidobatrachus llanensis* has a synapomorphy represented by character 44 (anterior and posterior dorsal shields, Fig. 4d).

Although this cladistic analysis could be improved by increasing the size of the data set of characters or by more extensive taxon sampling, the obtained hypothesis of phylogenetic relationships is sufficient to discuss intergeneric variation of selected traits of ceratophryines.

Skull shape variation

Skull shape variation in ceratophrynines

In the analysis of dorsal skull landmarks, RW1, RW2, and RW3 accounted for 72.13% of the variation (RW1 = 40.26%, RW2 = 19.62%, and RW3 = 12.25%). Relative warp values are given in Table 1. RW1 versus RW2 scatterplot reflects trajectories where lower values of RW1 are exhibited

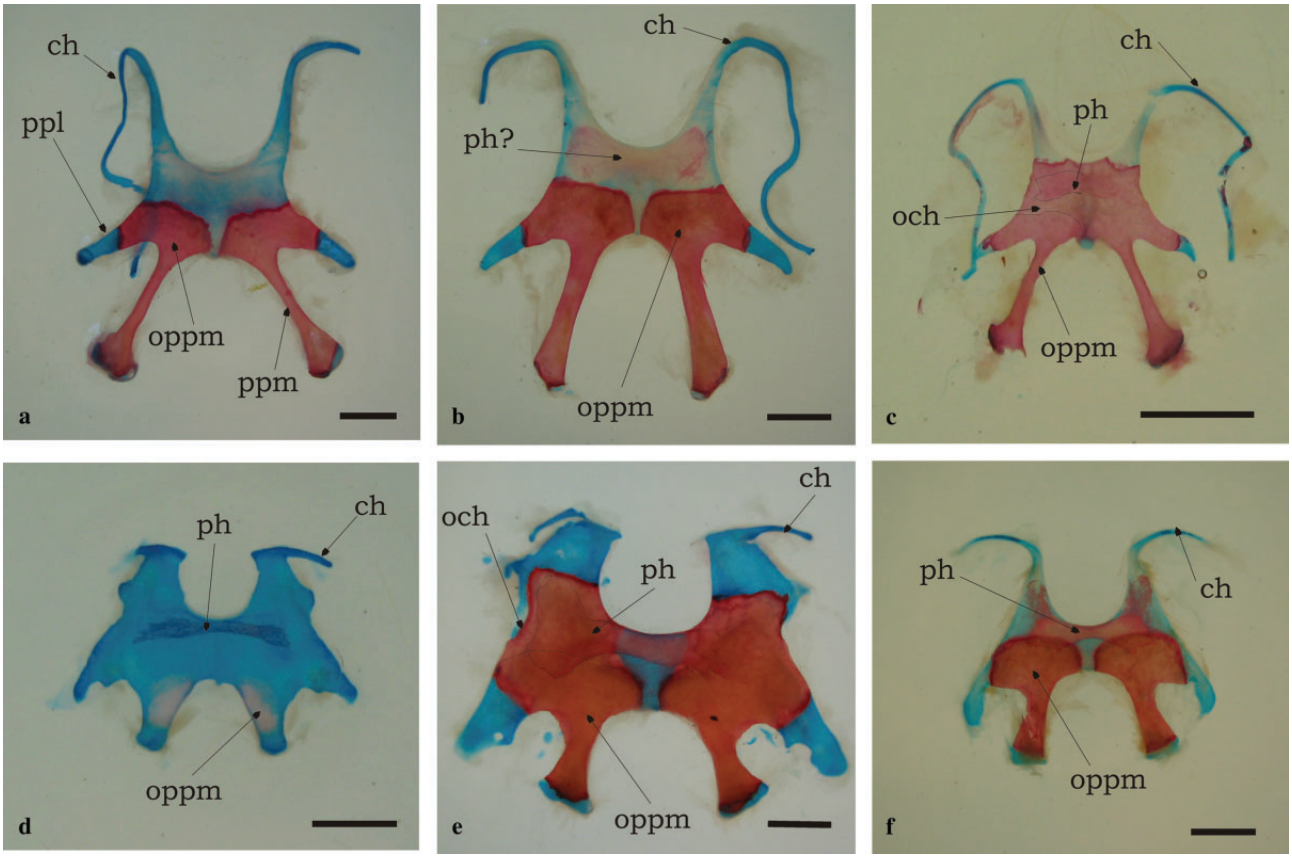

Fig. 3. Hyoid apparatus in ceratophryines is wide, lacks anterior and anterolateral processus, and has long and stout posterolateral processes. (a) *Ceratophrys cranwelli*, male (SVL = 80.36 mm). Posteromedial processes are elongated and ceratohyalia are continuous. The ossification of the posteromedial processes invades the hyoid plate and the epiphysis of the posteromedial processes after metamorphosis. (b) *C. cranwelli*, female (SVL = 103 mm). There is a poorly stained transversal bar 'parahyoid-like' in the largest female of the sample. (c) *Chacophrys pierottii*, male (SVL = 50 mm). The ossification of the posteromedial processes is more extensive in the hyoid plate, and reaches the posterolateral processes, the hyoglossal sinus, and the origins of the ceratohyalia, but does not fuse medially. Ceratohyalia are continuous. The parahyoid is a flat bone attached to the underlying hyoid plate. (d) *Lepidobatrachus laevis*, froglet female (SVL = 50 mm). Differentiation of the parahyoid bone takes place after metamorphosis and precedes the posteromedial ossifications. Ceratohyalia are discontinuous. (e) *L. laevis*, female (SVL = 110 mm). This large specimen has strong hyoid skeleton, short and bulky posteromedial processes, and incomplete ceratohyalia. The ossification of posteromedial processes invades the hyoid plate reaching the hyoglossal sinus. The parahyoid bone attached to the ventral face of the hyoid plate is well developed. (f) *L. llanensis*, female (SVL = 78 mm). Ceratohyalia are discontinuous but longer than in *L. laevis*. The ossification of the posteromedial processes does not reach the hyoglossal sinus. Parahyoid bone is well developed. Bars equal 5 mm. *Abbreviations*: ch, ceratohyal; och, ossification of hyoid cartilage; oppm, ossification of posteromedial process; ph, parahyoid; ppm, posteromedial process; ppl, posterolateral process

by *Chacophrys*, *Ceratophrys*, and smaller specimens of *Lepidobatrachus* spp. (Fig. 5a). RW1 explains shape changes involving a decrease in skull length and an increase in skull width at positive values (Fig. 5b). RW2 describes variation in the upper jaw length and posterior skull width; negative values represent smaller specimens of *Lepidobatrachus* spp. (Fig. 5b).

The lower jaw landmark data show that lower jaw shapes vary among ceratophryines, with clear differences between *Lepidobatrachus* and *Chacophrys-Ceratophrys*. Relative warp values are listed in Table 1. RW1, RW2, and RW3 accounted for 89.76% of the variation (RW1 = 56.98%, RW2 = 21.38%, and RW3 = 11.40%). RW1 versus RW2 scatterplot reflects trajectories where negative values of RW1 are exhibited by *Chacophrys*, *Ceratophrys*, and smaller specimens of *Lepidobatrachus* spp. (Fig. 5c). RW1 explains shape changes involving an increase of the length of the dentary and angulosplenial concomitant with a decrease in the length of the skull, from negative to positive values (Fig. 5d). RW2 displays variation in the relative position of lower jaw articulation with respect to the neurocranial articulation, from an anterior to a posterior position (Fig. 5d).

Skull shape variation among ceratophryines and other anurans

In dorsal skull, RW1, RW2, and RW3 comprised 59.80% of the variation (RW1 34.21%, RW2 14.54%, and RW3 11.05%). RW values for dorsal skull are listed in Table 2. RW1 versus RW2 scatterplot shows high values of RW1 for ceratophryines (Fig. 6a). Changes involve maxillary and squamosal length, skull width and length, and relative extension of nasal region relative to the consensus configuration (Fig. 6b). RW2 changes are reflected in squamosal and maxillary orientation, and nasal, frontoparietal, and maxillary lengths (Fig. 6b).

In lower jaw, RW1, RW2, and RW3 accumulated 87.16% of the variation (RW1 47.62%, RW2 23.39%, and RW3 16.15%). RW values for dorsal skull are listed in Table 2. RW1 versus RW2 scatterplot exhibits the extreme position of the ceratophryines with high positive values of RW1 (Fig. 6c).

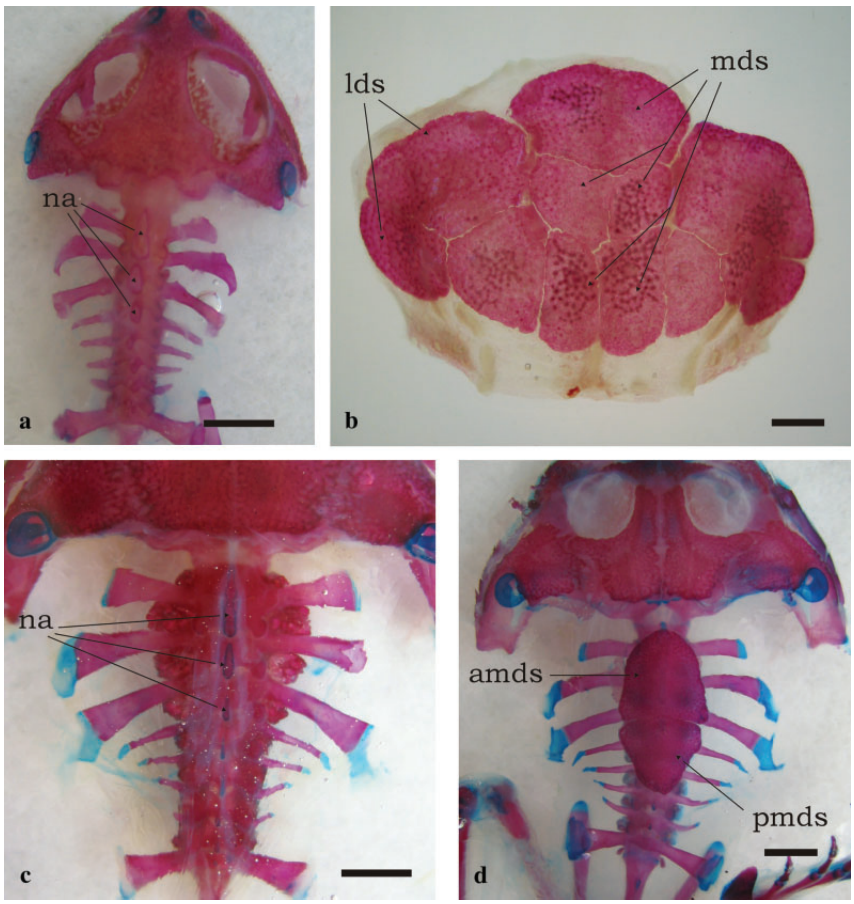

Fig. 4. Dorsal shields overlaying the presacral vertebrae among ceratophryines. (a) *Chacophrys pierottii*, male (SVL = 50 mm). Dorsal shields are absent. Neural spines of vertebrae II-IV are flattened. (b) *Ceratophrys cranwelli*, female (SVL = 103 mm), has composite dorsal shields from which medial and lateral shields cover vertebrae II–VII and their transverse processes. These shields develop at advanced juveniles stages. Metamorphosed specimens have flattened neural spines as was observed in adults of *Chacophrys*. (c) *Lepidobatrachus laevis*, male (SVL = 90 mm), lacks dorsal shields, and its neural spines are similar to those of *Chacophrys* and juvenile *Ceratophrys*. (d) *Lepidobatrachus llanensis*, juvenile (SVL = 67 mm). There are two medial dorsal shields, the anterior of which differentiates before metamorphosis. Tadpoles at larval stages 39–40 have already developed an anterior plate covering neural spines of vertebrae II and III, which reaches vertebra IV in juvenile stages. Shortly after, a posterior shield appears on neural spines of vertebrae V–VII. Bars equal 5 mm. *Abbreviations*: amds, antero-medial dorsal shield; lds, lateral dorsal shields; mds, medial dorsal shields, na, flatten neural arches; pdmds, postero-medial dorsal shield

Changes of shape resulting in positive values of RW1 imply elongation of lower jaw bones and skull length shortening (Fig. 6d). As you precede from negative to positive values for RW2 the jaw morphology changes from acuminated to a rounded lower jaw, and ceratophryines exhibit intermediate position in this axis (Fig. 6d).

Discussion

The Ceratophryinae clade

The Ceratophryinae was recognized by many studies (Reig and Limeses 1963; Lynch 1971; Maxson and Ruibal 1988; among others). Some authors proposed a familial status for *Chacophrys*, *Ceratophrys*, and *Lepidobatrachus* (Cei 1981) but at present, the group is considered part of the Ceratophryinae, with *Macrogenioglottus*, *Odontophrynus* and *Proceratophrys*, within the paraphyletic Leptodactylidae (Frost 2004).

Some features of ceratophryines seem to be primitive –e.g. tadpoles with 20 or 27 pairs of spinal nerves (Nishikawa and Wassersug 1989) or tadpoles having separate trigeminal and facial ganglia (Fabrezi and Chalabe 1997). Other ceratophryine's traits appear to be derived, or, at least, not present in those taxa considered basal – Ascaphidae, Leiopelmatidae, Bombinatoridae, and Discoglossidae – such as sculptured skulls, fangs (Fabrezi and Emerson 2003), monocuspid and non-pedicellate teeth (Smirnov and Vasil'eva 1995; Fabrezi 2001), etc.

Larval development in ceratophryines displays curious variation. Tadpoles of *Chacophrys* are typical pond larvae (Carrizo and Faivovich 1992); while *Ceratophrys* and *Lepidobatrachus* have carnivorous tadpoles with simplified internal oral structures (Wassersug and Heyer 1988), and a short alimentary tract with an adult-like stomach (Ruibal and Thomas 1988; Carroll et al. 1991; Ulloa Kriesler 2000). Further, *Lepidobatrachus* tadpoles have a symmetrical pair of large branchial openings (no siphons), derived from asymmetrical development resembling the sinistral spiracle of type 4 larvae (Ruibal and Thomas 1988), enlarged mouths without keratodonts and reduced beaks (Haas 2003), and external forelimb development. Thus, developmental larval variation in the ceratophryines may be one of the most important characteristics of their morphological evolution.

Peramorphosis is a developmental pattern of heterochrony that may be produced by an increase in rate (acceleration), a

Table 1. Singular values and percent explained for relative warps of lower jaw and dorsal skull analyses within ceratophrynines

Relative warp	Singular value	Percent explained (%)
Lower jaw		
RW1	0.35646	56.98
RW2	0.21835	21.38
RW3	0.15947	11.40
RW4	0.10048	4.53
RW5	0.07479	2.51
RW6	0.05053	1.14
RW7	0.04445	0.89
RW8	0.03866	0.67
RW9	0.03296	0.49
RW10	0.00532	0.01
Dorsal skull		
RW1	0.31483	40.26
RW2	0.21976	19.62
RW3	0.17365	12.25
RW4	0.14383	8.40
RW5	0.11143	5.04
RW6	0.09882	3.97
RW7	0.08540	2.96
RW8	0.07498	2.28
RW9	0.06805	1.88
RW10	0.05476	1.22
RW11	0.04263	0.74
RW12	0.03808	0.59
RW13	0.03238	0.43
RW14	0.02046	0.17
RW15	0.01502	0.09
RW16	0.01483	0.09

later offset time (hypermophosis), or an earlier onset time (predisplacement) of development of some structure (Reilly et al. 1997). Some osteological features, sometimes shared with other taxa, occur altogether in the ceratophryines and are excellent models for studies of peramorphosis and its influence on morphological evolution. Some features supporting the monophyly of ceratophryines in this paper were described as peramorphic traits among anurans. For example, character 12 (monocuspid teeth, Fabrezi 2001) and fangs (character 23, Fabrezi and Emerson 2003) seem to be integrated and correlated to dietary specialization (these fanged frogs eat large preys) and aggressive biting behaviour (Fabrezi and Emerson 2003). The following discussion points out other peramorphic features of ceratophryines.

Ossification of the hyoid is rare among anurans (Fig. 3). Usually, older specimens of some anuran taxa may have mineralization on the hyoid cartilage. The Bombinatoridae possess a pair of flat, plate-like endochondral bones in the hyoid (Trewavas 1933; Cannatella 1985). *Lepidobatrachus* spp. and *C. pierottii*, however, display an extended (hyper-) ossification of the posteromedial processes reaching the ceratohyalia. These ossifications progress during post-metamorphic growth and are more extensive in larger adults, showing a pattern of hypermorphosis. Among ceratophrynines, an increase in the degree of ossification of the hyoid could be interpreted as concomitant to an increase in size, or functionally as a need for a more robust lower jaw-cranium relation given the feeding ecology of ceratophryines.

Absence of the parahyoid bone is a neobatrachian synapomorphy (Ford and Cannatella 1993). A dermal V-shaped parahyoid is a synapomorphy for Discoglossidae (and convergent with *Pelodytes*) (Ford and Cannatella 1993), and a medial parahyoid appears in several taxa, such as *Ascaphus*, *Leiopelma*, *Barbourula*, *Bombina*, and *Rhinophrynus* (Cannatella 1985). Except for *Rhinophrynus*, all these taxa bear a discrete and small parahyoid bone, which is especially large in *Rhinophrynus* and also in the Ceratophryinae (Fig. 3c–f). de Beer (1937) described the Y-shaped parahyoid of *Polypterus* as a tendon ossification, probably of paired origin. This element does not properly belong to the hyobranchial skeleton, and may be homologous with the 'urohyal' of osteichtyan fishes and the parahyoid of Anura (de Beer 1937). In ceratophryines, the parahyoid can be considered a derived feature, but not a morphological novelty, because it is present in other anuran taxa (Müller and Wagner 1991).

Most anurans have continuous ceratohyalia, but *Lepidobatrachus* is the only neobatrachian taxon that has discontinuous ceratohyalia (Fig. 3d–f). Incomplete ceratohyalia – ceratohyalia lacking the intermediate pars – are present in *Rhinophrynus*, *Pelobates*, *Scaphiopus*, and *Pelodytes*, while the complete or almost complete absence of ceratohyalia in adults is a synapomorphy of Megophryidae (Cannatella 1985; Ford and Cannatella 1993).

Postcranial dorsal shields rarely occur among anurans (Fig. 4b,d). As the species having these ossifications are terrestrial, it was assumed they have been independently derived on at least three occasions as protective modifications (Trueb 1973). Dorsal shields were mentioned in *Lepidobatrachus asper*, *Ceratophrys aurita*, *Brachycephalus*, and dendrobatids (Trueb 1973). Dorsal shields are formed from the calcified layer of dermis, and could be vestigial structures corresponding to a dermal skeleton developed in ancestral amphibians, and may be associated with physiological functions (Toledo and Jared 1993). The calcified layer is better developed in dorsal skin and the concentration of material deposited increases with the age of the animal (Toledo and Jared 1993). An armor formed by dermal plates firmly attached by ligament to expanded neural spines was described among Permian dissorophids, and DeMar (1966) proposed a scenario of terrestrial conditions where thicken dermis allow less transfer of moisture though the skin. This functional significance seems to be a reasonable explanation for the presacral complex present in species of *Ceratophrys* typical of arid and semi-arid environments, such as *C. cranwelli* and *C. ornata*. Interestingly, the aquatic *L. llanensis* has poorly developed dorsal shields suggesting that they are being lost, due perhaps to lack of necessity for them.

Traits that represent reappearances of lost structures, imply a morphological integration that seems to arise from an underlying/quiescent developmental program that was conserved in the historical patterns shared by the ceratophryines. Reappearances in neobatrachians suggest that the loss of these structures did not mean the loss of the ability to form them. This ability was preserved in the developmental program of anurans and has re-emerged in the peramorphic ontogeny typical of ceratophryines.

Adult ceratophryines share a set of features that are formed during or immediately after metamorphosis – earlier than in other anuran taxa – such as appearance of tooth anlagen, paired fangs, and fusion of lower jaw bones (Table 3). Developmental pathways may be characterized as peramorphic with respect to other anurans (Table 3). Some of them involve reappearances of structures considered lost in the phylogeny of neobatrachians, suggesting that a peramorphic ontogeny may play a role in creating new designs without producing true morphological novelties.

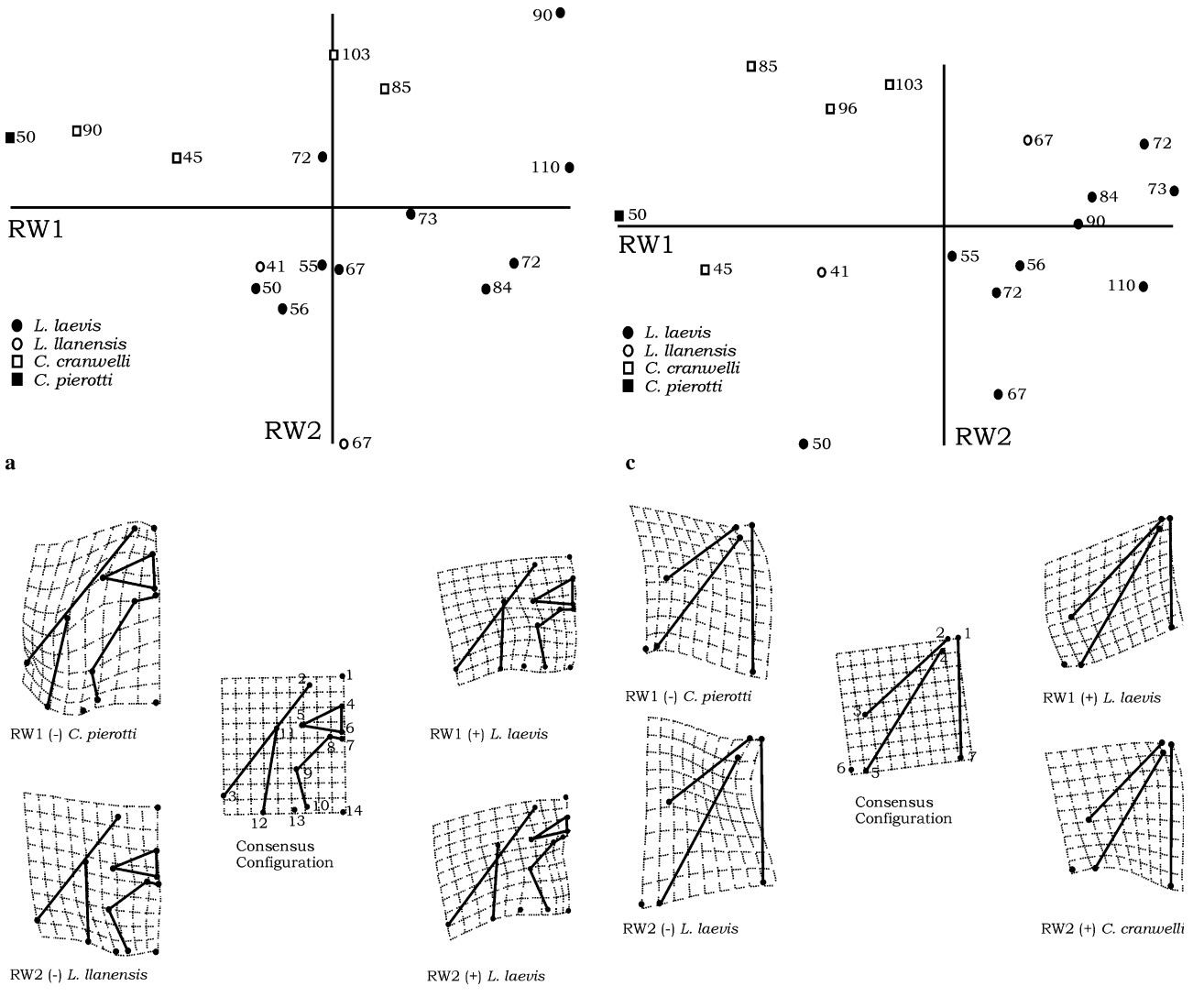

Fig. 5. Dorsal skull shapes within ceratophryines (a–b). (a) Scatterplott of RW2 versus RW1. Ontogenetic trajectories for *Lepidobatrachus laevis* proceed toward positive values of RW1 and RW2. Number associated with each point in the scatterplot is snout-vent length for that specimen in millimetres. Smaller specimens of *Lepidobatrachus laevis* show values of RW1 similar to those of larger specimens of *Ceratophrys cranwelli* suggesting changes in shape in *Lepidobatrachus laevis* are related with size (and age?). Extreme values in RW2 are represented by larger specimens of *Lepidobatrachus llanensis* and *Lepidobatrachus laevis*. (b) Schematic representation of extreme deformations along RW1 and RW2 in dorsal skull. Positive values of RW1 and RW2 in larger specimens of *Lepidobatrachus laevis* involve upper jaw enlargement, decreasing of skull length, and increase of posterior skull width relative to the consensus configuration. Negative values of RW1 represented in *Chacophrys pierottii* imply changes in the orientation and position of squamosal, increase in skull length, and increase of the frontoparietal extension respect to the consensus configuration. Negative values of RW2 exhibited by largest specimen of *Lepidobatrachus llanensis* are related to the posterior displacement of nasals and changes in the orientation of the squamosal relative to the consensus configuration. Lower jaw shapes within ceratophryines (c–d). (c) Scatterplott of RW2 versus RW1. Ontogenetic trajectories for *Lepidobatrachus* species proceed toward positive values of RW1 and RW2. Number associated with each point in the scatterplots is snout-vent length for that specimen in millimetres. Smaller specimens of *Lepidobatrachus* show values of RW1 similar to those of larger specimens of *Ceratophrys cranwelli* suggesting changes in shape in *Lepidobatrachus* are related with size (and age). Extreme values in RW2 are represented between smaller specimens of *Lepidobatrachus* and larger specimens of *Ceratophrys cranwelli*. (d) Schematic representation of extreme deformations along RW1 and RW2 in lower jaw. Positive values of RW1 in larger specimens of *Lepidobatrachus laevis* involve lower jaw enlargement and decrease of skull length relative to the consensus configuration. Negative values of RW1 represented in *Chacophrys pierottii* imply changes in the orientation and position of lower jaw respect of the consensus configuration. Positive values of RW2 exhibited by larger specimens of *Ceratophrys cranwelli* involve a decrease in the distance between lower jaw articulation and the skull longitudinal axis. Negative values of RW2 represent smaller specimens of *Lepidobatrachus laevis* where changes relative to the consensus configuration reflect a dentary shortening and changes in its orientation

Patterns of peramorphosis in skull shapes of ceratophrynines

The skull shape of *Lepidobatrachus* could be represented by a near circle, where the medial axis (ratio) is the skull length. In *Chacophrys* and *Ceratophrys*, skull lengths are longer than in *Lepidobatrachus*. These shape differences represent spatial and temporal repatterning involving major changes in the elongation of lower and upper jaws bones concomitant with posterior wideness of skull. *Chacophrys* and *Lepidobatrachus* skull shapes represent the extremes within the Ceratophryinae, while *Ceratophrys* may be

Table 2. Singular values and percent explained for relative warps of lower jaw and dorsal skull analyses among 50 anuran species

Relative warp	Singular value	Percent explained (%)
Lower jaw		
RW1	0.57297	47.62
RW2	0.40158	23.39
RW3	0.33363	16.15
RW4	0.21371	6.62
RW5	0.14640	3.11
RW6	0.10078	1.47
RW7	0.06964	0.70
RW8	0.06124	0.54
RW9	0.04674	0.32
RW10	0.02172	0.07
Dorsal skull		
RW1	0.69641	34.21
RW2	0.45407	14.54
RW3	0.39571	11.05
RW4	0.31965	7.21
RW5	0.30211	6.44
RW6	0.25992	4.77
RW7	0.22477	3.56
RW8	0.21371	3.22
RW9	0.19236	2.61
RW10	0.18386	2.38
RW11	0.17402	2.14
RW12	0.14313	1.45
RW13	0.13850	1.35
RW14	0.12114	1.04
RW15	0.11902	1.00
RW16	0.10633	0.80
RW17	0.09567	0.65
RW18	0.07858	0.44
RW19	0.07353	0.38
RW20	0.06193	0.27
RW21	0.05398	0.21
RW22	0.04276	0.13
RW23	0.03788	0.10
RW24	0.03160	0.07

considered an intermediate. As froglets and juveniles, the skull shapes of *Lepidobatrachus* are similar to *Ceratophrys*. The most remarkable change in the adult skull shape of *Lepidobatrachus* is the displacement of the lower jaw articulation posterior to the occipital joint.

Among anurans, the distinctiveness of the skull shape of ceratophryines is evident and reflects peramorphosis in the ontogeny of the group. TPS analyses of shape among a sample of 50 anuran taxa emphasized differences between ceratophryines and other frogs. Yeh (2002) described changes in skull shapes among anurans where the increase of growth of upper and lower jaws reflects more ontogenetic changes. As described here, ceratophryine characteristics of elongated jaws with a decrease in skull length result in their unique skull morphology. In dorsal view, RW1 versus RW2 scatterplots placed skull shape of *Pyxicephalus adspersus* near the ceratophrynines, but not in the extreme position of *Lepidobatrachus* (Fig. 7a). This is expected because *P. adspersus* has developed cranial exostosis via an extension of the squamosals, maxillaries, and frontoparietals that has resulted in an overall skull shape similar to the ceratophryines. Skull shapes in *Ceratophrys* and *Lepidobatrachus* are consequences of a strong divergence from the developmental patterns of the typical anuran.

Despite the fact that individual traits in jaws and hyoid apparatus are shared by ceratophryines and other taxa of anurans, the way in which they are integrated in the skull of the Ceratophryinae defines unique morphologies where developmental patterns of peramorphosis drive changes toward unusual directions.

The comparative data support the hypothesis of the monophyly of the Ceratophryinae. They share a particular set of morphological features resulting from patterns of peramorphosis. Some of the features represent ancient characters that have been considered lost in the neobatrachian evolution. Diversification in the group is limited to three genera, with no more than 15 species, suggesting that as an evolutionary process, peramorphosis is not particularly significant in terms of species diversification, but is able to produce morphological evolution. The genus *Lepidobatrachus* could be considered the extreme of ceratophrynine's morphology. Comprehension of peramorphic development is necessary to elucidate the association between development, growth, and evolution. The Ceratophryinae represent an appropriate subject for such studies.

Acknowledgements

I thank numerous colleagues. Raymond Laurent and Richard Tinsley gave me African specimens from their personal collections, which are deposited in the Museo de Ciencias Naturales (Universidad Nacional de Salta). Richard Wassersug provided helpful comments on an earlier draft of the manuscript. Fernando Lobo collaborated with the cladistic analyses. Carlos Infante carefully read to improve the English writing and added suggestions for a constructive discussion. Natalia von Ellenrieder read the last version. Virginia Abdala, Javier Goldberg, Adriana Jerez, and Maria Inés Martinez contributed with observations on the manuscript. This research was supported by CONICET (PEI 6094/PIP 2829 to M.F).

Resumen

Evolución morfológica en Ceratophryinae (Anura, Neobatrachia).

Numerosos estudios han enfatizado la importancia en la generación de novedades de aquellas heterocronías que implican paedomorfosis en los anuros. En este trabajo se analiza la variación morfológica en *Chacophrys*, *Ceratophrys* y *Lepidobatrachus*, géneros que se reúnen en la sufamilia Ceratophryinae de Leptodactylidae. Estos presentan rasgos particulares que reflejan tasas de desarrollo incrementado y ofrecen la posibilidad de explorar su variación a nivel intergenérico. La monofilia de los Ceratophryinos es soportada en el análisis de caracteres morfológicos. A diferencia de otros anuros, donde los rasgos característicos son resultado de ausencias o reducciones, en la morfología de los ceratophryinos aparecen todos los rasgos observados en la variación intraordinal, algunos de los cuales se encuentran exageradamente desarrollados y/o representan reapariciones de caracteres que se consideraban perdidos entre los neobatracios. La forma de la cabeza, que también refleja un patrón de peramorfosis, es otra característica distintiva que presentan estos anuros. Representa la integración del conjunto de variación cuantitativa que ocurre a nivel de los distintos elementos craneales y tiene en común el acortamiento del cráneo y un alargamiento concomitante de las mandíbulas. Este estudio evidencia el papel de la peramorfosis en la evolución morfológica de un clado monofilético de anuros.

References

de Beer, G. R., 1937: The Development of the Vertebrate Skull. Oxford: Clarendon Press.

Bookstein, F. L., 1991: Morphometric Tools for Landmark Data: Geometry and Biology. New York: Cambridge University.

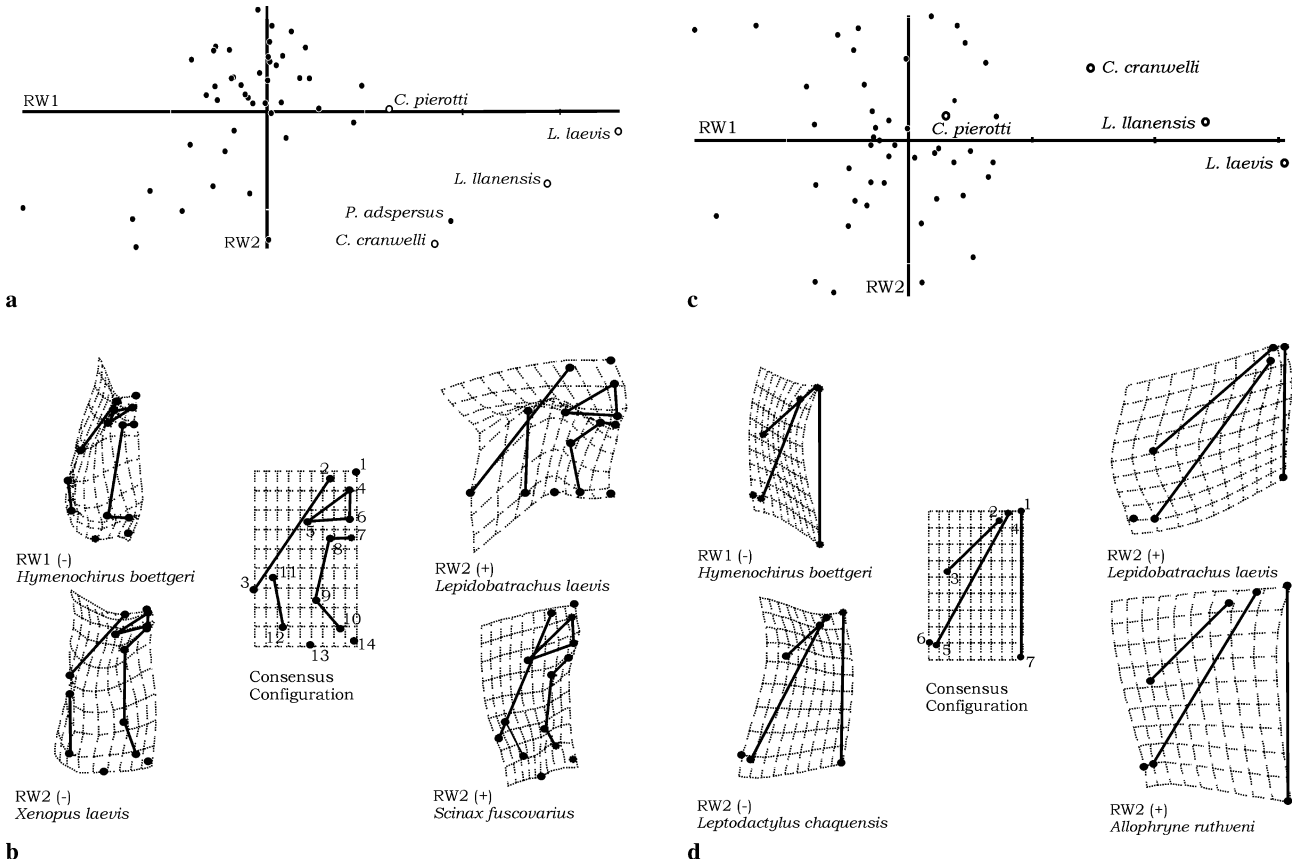

Fig. 6. Dorsal skull shape variation among 50 species of anurans (a–b). (a) Scatterplot of RW1 versus RW2. Ceratophryines and *Pyxicephalus adspersus* share distinctive high values of RW1. Along RW1, trajectories for ceratophryines species proceed toward positive values of RW1 with the highest value for *L. laevis*. Variation in RW2 placed *Ceratophrys cranwelli* and *Pyxicephalus adspersus* with negative values. Most anuran taxa present intermediate values of RW1 and positive values for RW2. (b) Extreme deformations relative to the consensus configuration in RW1 and RW2. Changes in shape toward positive values of RW1 represented by *L. laevis*, have implied enlargement of maxillaries and squamosals, decrease in the skull length, an increase of the width in posterior skull and nasals extension. *Hymenochirus boettgeri* displays lowest value of RW1 and changes involved in dorsal skull shape are upper jaw bones shortening, and increase of the frontoparietal extension. Positive values of RW2 exhibited by *Scinax fuscovarius* integrate changes relative to maxillaries enlargement, orientation of squamosals and nasals, and decrease in the posterior skull width. Negative values of RW2 represented by *Xenopus laevis* correspond to maxillaries and nasals shortening, frontoparietal enlargement, changes in the orientation of squamosal and an increase of the posterior skull width. Lower jaw shapes variation among 50 species of anurans (c–d). (c) Scatterplot of RW1 versus RW2. Along RW1, trajectories for ceratophryines species proceed toward positive values of RW1; but *Chacophrys* is not distinctive from other anurans. Variation in RW2 placed ceratophryines among most anuran taxa in intermediate values. (d) Extreme deformations relative to the consensus configuration in RW1 and RW2. Changes in shape toward positive values of RW1 represented by *Lepidobatrachus laevis*, have implied enlargement of lower jaw and a strong decrease in the skull length and width. *Hymenochirus boettgeri* displays the lowest value of RW1 and changes are lower jaw bones shortening, increase of skull length and decrease of skull width. Positive values of RW2 exhibited by *Allophryne ruthveni* integrate enlargement of angulosplenial and skull length concomitant with an increase of the width of the lower jaw. Negative values of RW2 represented by *Leptodactylus chaquensis* correspond to dentaries shortening, enlargement of skull length and a decrease of the lower jaw width

Cannatella, D. C., 1985: A phylogeny of primitive frogs (Archaeobatracians). PhD Dissertation. Lawrence, KS: The University of Kansas.

Carrizo, G. R.; Faivovich, J., 1992: Descripción de la larva de *Chacophrys pierottii* (Vellard, 1948) (Leptodactylidae, Ceratophryinae). Alytes **10,** 81–89.

Carroll Jr, E. J.; Seneviratne, A. M.; Ruibal, R., 1991: Gastric pepsin in an anuran larva. Dev. Growth Differ., **33,** 499–507.

Cei, J. M., 1981: Amphibians of Argentina. Monit. Zool. Ital. Monogr. **2,** 1–609.

Clarke, B. T., 1996: Small size in amphibians-its ecological and evolutionary implications. Symp. Zool. Soc. Lond. **69,** 201–224.

DeMar, R. E., 1966: The phylogenetic and functional implications of the armor of the Dissorophidae. Fieldiana: Geol. **16,** 55–88.

Duellman, W. E., 1993: Amphibians species of the world: additions and corrections. Univ. Kansas Mus. Nat. Hist. Spec. Publ. **21,** 1–372.

Fabrezi, M., 2001: Variación morfológica de la dentición en anuros. Cuad. herpetol. **15,** 17–28.

Fabrezi, M.; Chalabe, T., 1997: A review of the fusion of trigeminal and facial ganglia during ontogeny of some neobatrachian anuran. Alytes **15,** 1–12.

Fabrezi, M.; Emerson, S. B., 2003: Parallelism and convergence in anuran fangs. J. Zool., Lond. **260,** 41–51.

Ford, L.; Cannatella, D. C., 1993: The major clades of frogs. Herpetol. Monogr. **7,** 94–117.

Frost, D. R., 2004: Amphibian Species of the World: An Online Reference. Version 3.0, Accessible at: http://research/amnh.org/herpetology/amphibian/index.php on 22 August 2004. New York, USA: American Museum of Natural History.

Goloboff, P. A., 1993: Estimating character weights during tree search. Cladistics **9,** 83–91.

Table 3. Comparison of relative timing of developmental events between ceratophryines and other anurans. Major features of ceratophryines are already developed during metamorphosis. Most fanged frogs have marked sexual dimorphism in relative fang sizes, in contrast, in ceratophryines the presence of fangs seems to be correlated with dietary specialization (Fabrezi and Emerson 2003). Data from this study and previous studies mentioned in the table.

Developmental features	Ceratophryines	Other anurans
Appearance of tooth anlagen (Smirnov and Vasil'eva 1995; Vasil'eva 1997; Wild 1997, 1999; Sheil 1999; Fabrezi 2001)	Beginning of metamorphosis	Beginning of metamorphosis in *Pyxicephalus adspersus*, end of metamorphosis or right after in *Pelobates fuscus*, *Pipa pipa* and *Bombina* spp.
Differentiation of paired fangs (Wild 1999; Fabrezi and Emerson 2003)	Beginning of metamorphosis	Juvenile stages in some ranid frogs
Fusion of dentary and mentomeckelian (Fabrezi and Emerson 2003)	At metamorphosis or immediately after	Juveniles stages in some ranid frogs
Ossification of posteromedial processes (Wild 1997, 1999)	Immediately after metamorphosis in *Ceratophrys* and *Chacophrys*, juveniles stages in *Lepidobatrachus* spp.	Immediately after metamorphosis
Parahyoid ossification (Ridewood 1897)	Immediately after metamorphosis in *Lepidobatrachus* spp., adults in *Chacophrys*, occasionally older specimens of *Ceratophrys*	After metamorphosis in *Pelodytes punctatus*
Dorsal shields	Larval stages in *Lepidobatrachus llanensis*, adults of *Ceratophrys cranwelli*	? (unknown)

Goloboff, P.; Farris, J.; Nixon, K., 2003. T.N.T.: Tree Analysis Using New Technology. Program and documentation available from the authors, and http://www.amuc.dk/public/phylogeny.

Gosner, K., 1960: A simplified table for staging anuran embryos and larvae with notes on identification. Herpetologica **16,** 183–190.

Haas, A., 2003: Phylogeny of frogs as inferred from primarily larval characters (Amphibia: Anura). Cladistics **19,** 23–89.

Hanken, J., 1993: Model systems versus outgroups: alternative approaches to the study of head development and evolution. Amer. Zool. **33,** 448–456.

Hanken, J.; Jennings, D. H.; Olsson, L., 1997: Mechanistic basis of life-history evolution in anuran amphibians: direct development. Am. Zool. **37,** 195–207.

Lanyon, S. M., 1985: Detecting internal inconsistencies in distance data. Syst. Zool. **34,** 397–403.

Laurent, R. F., 1986: Souss classe lissamphibiens (Lissamphibia). Systématique. In: Grassé, P.-P.; Delsol, M. (eds), Traité de Zoologie. Anatomie, Systématique, Biologie. Paris: Tome XIV, Batraciens, Fasc. 1B. Masson, pp. 594–798.

Lynch, J., 1971: Evolutionary relationships, osteology, and zoogeography of leptodactyloid frogs. Univ. Kansas Mus. Nat. Hist. Misc. Publ. **53,** 1–238.

Maxson, L. R.; Ruibal, R., 1988: Relationships of frogs in the subfamily Ceratophryinae. J. Herpetol. **22,** 228–231.

Müller, G. B.; Wagner, G. P., 1991: Novelty in evolution: restructuring the concept. Annu. Rev. Ecol. Syst. **22,** 229–256.

Nishikawa, K.; Wassersug, R. J., 1989: Evolution of spinal nerve number in anuran larvae. Brain Behav. Evol. **33,** 15–24.

Reig, O. A.; Limeses, C. E., 1963: Un nuevo género de anuros ceratophrínidos del distrito chaqueño. Physics **24,** 113–128.

Reilly, S. M.; Wiley, E. O.; Meinhardt, D. J., 1997: An integrative approach to heterochrony: the distinction between interspecific and intraspecific phenomena. Biol. J. Linn. Soc. **60,** 119–143.

Ridewood, W. G., 1897: On the structure and development of the hyobranchial skeleton of the parsley-frog *Pelodyts punctatus*. Proc. zool. Soc. Lond. **1897,** 577–595.

Rohlf, F. J., 2003: tpsRelw, Relative Warps Analysis, version 1.37, available at: http://life.bio.sunysb.edu/morph/morphmet.html.

Rohlf, F. J., 2004a: tpsDig 1.4, available at: http://life.bio.sunysb.edu/morph/morphmet.html.

Rohlf, F. J., 2004b: tpsSpline, Thin-Plate Spline, version 1.19, available at: http://life.bio.sunysb.edu/morph/morphmet.html.

Ruibal, R.; Thomas, E., 1988: The obligate carnivorous larvae of the frog *Lepidobatrachus laevis* (Leptodactylidae). Copeia **1988,** 591–604.

Sheil, A. C., 1999: Osteology and skeletal development of *Pyxicephalus adspersus* (Anura: Ranidae: Raninae). J. Morphol. **240,** 49–75.

Smirnov, S. V.; Vasil'eva, A. B., 1995: Anuran dentition: development and evolution. Russ. J. Herpetol. **2,** 120–128.

Toledo, R. C.; Jared, C., 1993: The calcified dermal layer in anurans. Comp. Biochem. Physiol. **104A,** 443–448.

Trewavas, E., 1933: The Hyoid and Larynx of the Anura. Trans. R. Phil. Soc. Lond. **222,** 401–527.

Trueb, L., 1973: Bones, frogs, and evolution. In: Vial, J. L. (ed.), Evolutionary Biology of the Anurans: Contemporary Research on Major Problems. Columbia, MO: University of Missouri Press, pp. 65–132.

Ulloa Kriesler, Z. E., 2000: Metamorfosis del aparato digestivo de larvas carnívoras de *Ceratophrys cranwelli* (Anura: Leptodactylidae). Cuad. Herpetol. **14,** 105–116.

Vasil'eva, A. B., 1997: The role of pedomorphosis in the formation of the tooth system in Anura with the example of the fire-billed toads (*Bombina*, Discoglossidae). Doklady Akademii Nauk. **354,** 566–568.

Wassersug, R. J., 1976: A procedure for differential staining of cartilage and bone in whole formalin fixed vertebrates. Stain Technol. **51,** 131–134.

Wassersug, R. J.; Heyer, W. R., 1988: A survey of internal oral features of leptodactyloid larvae (Amphibia: Anura). Smithson. Contrib. Zool. **457,** 1–99.

Wild, E. R., 1997: Description of the adult skeleton and developmental osteology of the hyperossified horned frog, *Ceratophrys cornuta* (Anura: Leptodactylidae). J. Morphol. **232,** 169–206.

Wild, E. R., 1999: Description of the chondrocranium and osteogenesis of the chacoan burrowing frog, *Chacophrys pierottii* (Anura: Leptodactylidae). J. Morphol. **242,** 229–246.

Yeh, J., 2002: The evolution of development: two portraits of skull ossification in pipoid frogs. Evolution **56,** 2484–2498.

Author's address: Marissa Fabrezi, CONICET – Instituto de Bio y Geociencias y Museo de Ciencias Naturales, Universidad Nacional de Salta. Mendoza 2, 4400-Salta, República Argentina. E-mail: mfabrezi@aol.com

Appendix 1.

Specimens of Ceratophryinae for osteological examination of selected traits

Ceratophrys cranwelli Barrio, 1980: MCN 188 (male 80 mm); MCN 206 (male 85 mm); MCN 206 (female 96 mm), MCN 819 (female 103 mm); MCN 819 (male 80 mm); MCN 819 (male 81 mm); MCN 933 (juvenile 45 mm).

Chacophrys pierottii (Vellard, 1948): FML 2651 (male, 50 mm).

Lepidobatrachus laevis Budgett, 1899: MCN 109 (male 72 mm); MCN 109 (male 84 mm); MCN 695 (female 110 mm); MCN 815 (male 90 mm); MCN 831 (female 72 mm); MCN 831 (male 67 mm); MCN 931 (female 56 mm); MCN 934 (male 55 mm); MCN 935 (male 73 mm); MCN 936 (male 50 mm).

Lepidobatrachus llanensis (Duméril and Bibron, 1841): MCN 081 (female 78 mm); MCN 667 (male 67 mm); MCN 932 (metamorphic stages 45 and 46); MCN 567 (15 tadpoles at larval stages 38–42).

Specimens examined for cladistic analyses (*), and specimens for thin-plate spline morphometric analyses (**)

Allophrynidae: *Allophryne ruthveni* Gaige, 1926: MNHN 00539 (24 mm) *, **.

Arthroleptidae: *Arthroleptis adolfifriederici* Nieden, 1911: MCN 822 (female, 39 mm) *, **; *Arthroleptis poecilonotus* Peters, 1863: MCN 950 (male) *; *Arthroleptis variabilis* Matschie, 1893: MCN 938 (female) *; *Cardioglossa cyaneospila* Laurent, 1950: MCN 821 (female, 35 mm) *; **; *Cardioglossa leucomystax* (Boulenger, 1903): MCN 939 (female) *; *Schoutedenella pyrrhoscelis* (Laurent, 1952): MCN 827 (female, 19 mm) *, **; *Schoutedenella sylvatica* Laurent, 1954: MCN 940 (female) *; *Schoutedenella lameerei* (Witte, 1921): MCN 941 (male) *; *Schoutedenella schubotzi* (Nieden, 1911): MCN 942 (female) *.

Astylosternidae: *Astylosternus diadematus* Werner, 1898: FML 3215 (43 mm) *, **.

Bombinatoridae: *Bombina variegata* (Linnaeus, 1758): MCN 810 (37 mm) *, **.

Bufonidae: *Bufo granulosus* Spix, 1824: MCN 796 (male, 53 mm) *, **; *Bufo variegatus* (Günther, 1870): MCN 012 (male, 35 mm) *, **; *Melanophryniscus rubriventris* (vellard, 1947): MCN 071 (female, 42 mm) *, **.

Hylidae: *Flectonotus fitzgeraldi* (Parker, 1934): MCN 017 (27 mm) *, **; *Hyla andina* Müller, 1924: MCN 937 (male, 43 mm) *, **; *Hyla nana* (Boulenger, 1889): MCN 791 (male, 22 mm) *, **; *Hyla rivularis* Taylor, 1952: MCN 013 (34 mm) *, **; *Phyllomedusa lemur* Boulenger, 1882: MCN 012 (male 35 mm) *, **; *Phyllomedusa sauvagii* Boulenger, 1882: MCN 795 (male, 71 mm) *, **; *Pseudis paradoxus* (Linnaeus, 1758): MCN 812 (female, 42 mm) *, **; *Scinax fuscovarius* (Lutz, 1925): MCN 813 (female, 31 mm) *, **.

Hyperoliidae: *Afrixalus fulvovittatus* (Cope, 1861): MCN 943 (26 mm), *, **; *Hyperolius castaneus* Ahl, 1931: MCN 833 (female, 29 mm) *, **; *Hyperolius kivuensis* Ahl, 1931: MCN 804 (female, 32 mm) *. **; *Kassina senegalensis*(Duméril and Bibron, 1841): MCN 823 (42 mm) *, **; *Leptopelis christyi* (Boulenger, 1912): MCN 829 (female, 44 mm) *, **; *Opisthothylax immaculatus* (Boulenger, 1903): MCN 825 (29 mm) *, **; *Phlyctimantis verrucosus* (Boulenger, 1912): MCN 832 (52 mm), *, **.

Leptodactylidae: *Ceratophrys cranwelli*: MCN 206 (male 85 mm) **; MCN 206 (female 96 mm) **; MCN 819 (female 103 mm) *, **; MCN 933 (juvenile 45 mm) **. *Chacophrys pierottii* FML 2651 (male, 50 mm) *, **; *Lepidobatrachus laevis*: MCN 109 (male 72 mm) **; MCN 109 (male 84 mm) **; MCN 695 (female 110 mm) *, **; MCN 815 (male 90 mm) **; MCN 831(female 72 mm) **; MCN 931 (female 56 mm) **; MCN 934 (male 55 mm) **; MCN 935 (male 73 mm) **; MCN 936 (male 50 mm), ** (female, 110 mm); *Lepidobatrachus llanensis*: MCN 667 (male 67 mm) *, **; MCN 932 (metamorphic stages 45 and 46) **; *Leptodactylus bufonius* Boulenger, 1894: MCN 074 (female, 58 mm) *, **; *Leptodactylus chaquensis* Cei, 1950: MCN 039 (female, 87 mm) *, **; *Leptodactylus latinasus* Jiménez de la Espada, 1875: MCN 083 (female, 31 mm) *, **; *Odontophrynus americanus* (Duméril and Bibron, 1841): MCN 105 (female, 55 mm) *, **; *Physalaemus biligonigerus* (Cope, 1861): MCN 802 (female, 38 mm) *, **; *Pleurodema bufonina* Bell, 1843: MCN s/n (44 mm) *, **.

Microhylidae: *Phrynomantis bifasciatus* (Smith, 1847): MCN 830 (54 mm) *, **.

Petropedetidae: *Phrynobatrachus acutirostris* Nieden, 1913: MCN 951, *; *Phrynobatrachus dendrobates* (Boulenger, 1919): MCN 826 (30 mm) *, **; *Phrynobatrachus natalensis*: MCN 824 (27 mm) **; *Phrynobatrachus petropedetoides* Ahl, 1924: MCN 948, *; *Phrynobatrachus sulfureogularis* Laurent, 1951: MCN 949, *; *Phrynobatrachus versicolor* Ahl, 1924: MCN 828 (female, 27 mm) *, **.

Pipidae: *Hymenochirus boettgeri* (Tornier, 1896): MCN 811 (male, 33 mm) *, **; *Xenopus laevis* (Daudin, 1802): MCN 944 (female, 56 mm) *, **.

Ranidae: *Afrana angolensis* (Bocage, 1866): MCN 803 (male 80, mm) *, **; *Amnirana albolabris* (Hallowell, 1856): MCN 805 (female, 64 mm) *, **; *Aubria subsigillata* (Duméril, 1856): MCN 835 (female, 66 mm) *, **; *Conraua crassipes* (Buchholz and Peters *In* Peters, 1875): MCN 834 (male, 51 mm) *, **; *Hoplobatrachus occipitalis* (Günther, 1858): MCN 807 (female, 112 mm) *, **; *Ptychadena chrysogaster* Laurent, 1954: MCN 946, *, *Ptychadena christyi* (Boulenger, 1919): MCN 947, *; *Ptychadena mascareniensis* (Duméril and Bibron, 1841): MCN 820 (female, 40 mm) *, **; *Ptychadena uzungwensis* (Loverdige, 1932): MCN 945, *; *Pyxicephalus adspersus* Tschudi, 1838: MCN 806 (female, 186 mm) *, **.

Rhacophoridae: *Chiromantis rufescens* (Günther, 1869): MCN 831 (52 mm) *, **.

Rhinodermatidae: *Rhinoderma darwinii* Duméril and Bibron, 1841: MCN 020 (23 mm) *, **.

Scaphiopodidae: *Scaphiopus couchii* Baird, 1854: MCN 808 (male, 58 mm) *, **; *Spea bombifrons* (Cope, 1863): MCN 809 (female, 58 mm) *, **.

Abbreviations of museums: MNHN, Museo Nacional de Historia Natural, Montevideo, Uruguay; FML, Instituto de Herpetología, Fundación Miguel Lillo, Tucumán, Argentina; MCN, Museo de Ciencias Naturales, Universidad Nacional de Salta, Argentina.

Appendix 2. List of characters examined in the cladistic analysis

0. Nasal shape: 0 – triangular and large; 1 – reduced to a narrow slip of bone. *1. Nasals medial contact:* 0 – fused or in contact; 1 – moderately to widely separated. *2. Cranial exostosis:* 0 – absent; 1 – present. *3. Dorsal exposure of sphenethmoid:* 0 – invisible dorsally; 1 – visible dorsally. *4. Ventral configuration of sphenethmoid:* 0 – a single bone; 1 – consisting of two elements. *5. Frontoparietals medial contact:* 0 – no medial contact; 1– slightly separated; 2 – sutured or fused. *6. Supraobital alae:* 0 – absent; 1 – present. *7. Frontoparietals:* 0 – parallel sided; 1–the posterior end is wider than the anterior. *8. Parieto–squamosal arch:* 0 – absent; 1 – present. *9. Interfrontal:* 0 – absent; 1 – present. *10. Otic ramus of squamosal:* 0 – absent or rudimentary; 1 – overlapping crista parotica; 2 – overlapping crista parotica and otocccipital. *11. Zygomatic ramus of squamosal:* 0 – short or absent; 1 – moderately developed; 2 – long; reaching maxilla. *12. Teeth:* 0 – absent; 1 – bicuspid; 2 – monocuspid. *13. Shape of anterior end of maxillary:* 0 – concave; 1 – straight. *14. Pars palatina of premaxilla:* 0 – present; 1 – reduced; 2 – absent. *15. Orientation of alaris processes of premaxillae:* 0 – parallel; 1 – divergent. *16. Pars facialis of maxilla:* 0 – low; 1 – high. *17. Anterior ramus of pterygoid:* 0 – long; reaching the antorbital planum; 1 – short. *18. Pterygoid rami:* 0 – well differentiated; 1 – posterior and medial rami forming a plate. *19. Prevomer:* 0 – absent or impair; 1 – incomplete, without odontophore; 2 – complete. *20. Anterior process of prevomer:* 0 – long, reaching the articulation premaxilla–maxilla; 1 – short. *21. Quadratojugal:* 0 – absent or reduced; 1– entire, but not contacting maxilla; 2 – articulated or fused maxilla. *22. Palatine:* 0 – absent; 1: present. *23. Fangs in lower jaw:* 0 – absent; 1 – forming a plate of dentary; 2 – a spur–like projection formed by dentary and mentomeckelian bones. *24. Mentomeckelian bone:* 0 – absent; 1 – different from dentary; 2 – fused to dentary. *25. Ceratohyalia:* 0 – continuous; 1 – discontinuous. *26. Ceratohyalia processes:* 0 – absent; 1 – anteromedial processes; 2 – anteromedial and anterolateral processes; 2 – anteromedial and anterolateral processes fused in an arch. *27. Anterolateral process of hyoid plate:* 0 – absent; 1 – pointed; 2 - dilated distally; 3 – expanded; the base is extremely broad. *28. Posterolateral process of hyoid plate:* 0 – absent; 1 – present. *29. Posteromedial process ossification:* 0 – ossification present on a cartilaginous stalk; 1 – ossification abut directly on the hyoid; 2 – ossification invades the hyoid. *30. Posteromedial epiphyses:* 0 – cartilaginous; 1 – ossified. *31. Posteromedial ridge of posteromedial process:* 0 – absent; 1 – present. *32. Parahyoid bone:* 0 – absent; 1 – small ossification; 2 – transversal bar. *33. Endochondral ossifications in the hyoid:* 0 – absent; 1 – present. *34. Number of presacral vertebrae:* 0 – eight; 1 – seven. *35. Shape of 8th presacral vertebra:* 0 – opisthocoelous; 1– procoelous; 2 – biconcave. *36. Cervical cotyle arrangement:* 0– contiguous; 1 – separated. *37. Sacral vertebra and urostile:* 0 – articulated; 1 – fused. *38. 8th presacra and sacral vertebra:* 0 – separated; 1 – fused. *39. Neural arches:* 0 – imbricate; 1 – no imbricate. *40. Neural spines:* 0 – low; 1– high; 2 – flatten. *41. Relative length of transverse processes:* 0 – decreasing gradually in caudal direction; 1 – decreasing abruptly from IV vertebra to caudal direction. *42. Sacral transverse processes:* 0 – widely expanded; 1 – moderately dilated; 2 – cylindrical. *43. Ribs:* 0 – absent; 1 – present. *44. Dorsal shields:* 0 – absent; 1 – two ossifications; anterior and posterior; 2 – complex formed by a set of plates. *45. Orientation of transverse processes of 8th presacral vertebra:* 0 – perpendicular to axial axis; 1 – markedly forward; 2 – absent. *46. Omosternon:* 0 – cartilaginous; 1 – ossified; not forked, 2 – ossified, forked; 4– absent. *47. Metasternon:* 0 – absent; 1 – cartilaginous; 2 – proximal ossified style. *48. Coracoid:* 0 – entire medial margin; 1 – perforated medial margin. *49. Clavicle:* 0 – well developed; 1 – reduced; 2 – absent. *50. Epicoracoid:* 0 – widely overlapping; 1 – slightly overlapping; 2 – fused; 3 – quite absent, coracoids medial union. *51. Scapula:* 0 – short; 1 – long. *52. Ilial shaft:* 0 – absent; 1 – present. *53. Epipubis:* 0 – absent; 1 – present. *54. Femoral crest:* 0 – absent; 1 – present. *55. Intercalary elements:* 0 – absent; 1 – present. *56. Tarsal sesamoidea:* 0 – absent; 1 – os cartilage sesamoidea; 2 – os sesamoidea tarsale. *57. Distal tarsal 3 and distal tarsal 2:* 0 – free; 1 – fused. *58. Distal tarsal 1:* 0 – absent; 1 – present. *59. Prehallux:* 0 – one spherical proximal element; 1 – two elements; the distal one enlarged; 2 – three or more elements; 3 – two elements; the distal one hypermorphic. *60. Shape of terminal phalanx of toe IV:* 0 – straight; 1 – curved. *61. Distal tip of terminal phalanx of toe IV:* 0 – knob–like; 1 – pointed; 2 – notched; 3 – T shaped; 4 – Y shaped. *62. Ventral spine of toe IV:* 0 – absent; 1 – present. *63. Subarticular sesamoidea of toes:* 0 – absent; 1 – present. *64. Postaxial carpals (ulnare and distals 5 and 4)*: 0 – unfused; 1 – ulnare free; 5 and 4 fused; 2 – ulnare free; 5, 4 and 3 fused; 3 – ulnare and 5 fused, 4 free. *65. Preaxial carpals (element Y and distal 2):* 0 – unfused, 1 – 2 and Y fused; 2 – element Y, distal 3 and 3 fused. *66. Prepollex:* 0 – one spherical proximal element; 1 – two elements, the distal one enlarged; 2 – three or more elements; 3 – two elements, the distal one hypermorphic. *67. Shape of terminal phalanx of finger IV:* 0 – straight; 1 – curved. *68. Distal tip of terminal phalanx of finger IV:* 0 – knob–like; 1 – pointed; 2 – notched; 3 – T shaped; 4 – Y shaped. *69. Ventral spine of finger IV:* 0 – absent; 1 – present. *70. Subarticular sesamoidea of finger IV:* 0 – absent; 1 – present. *71. Carpal torsion:* 0 – absent; 1 – present. *72. Parotoid glands:* 0 – absent; 1 – present. *73. Bidder organ:* 0 – absent; 1 – present. *74. Development:* 0 – direct; 1 – larval. *75. Spiracle:* 0 – pair; 1 – single and sinistral; 2 – single and medial; 3 – single, medial and posterior. *76.Keratinized jaws:* 0 – absent; 1 – present. *77. Keratodonts:* 0 – absent; 1 – present.*78. Sexual dimorphism in size:* 0 – females larger than males; 1 – females equal or smaller than males. *79. Sexual dimorphism in finger length:* 0 – absent; 1 – present. *80. Heterochronic traits related to size:* 0 – absent; 1 – noticeable paedomorphic traits; 2 –noticeable peramorphic traits.

Appendix 3. Species and character states for cladistic analyses

Bombina variegata	1101010101001100000212001003110011001000000101010000001000110000001000000001211000
Arthroleptis adolfifriederici	0101110100111101000112101013010000011001002000210021100011110001111000011000???010
Arthroleptis poecilonotus	0101010100111100000112101013010000011001002000210021100011130001111000011000???010
Arthroleptis variabilis	0101010100111101000112101013010000011001002000210021100011110001111000011000???010
Astylosternus diadematus	0001020100111100110212101012110000020001002000210021100011131110201000010011110000
Afrixalus fulvovittatus	0001120100111100000112101022000000021001002001210020000101111210101121010011110001
Allophryne ruthveni	0101020000110110010110001002110000011001001000310001001001000300200030010011110000
Aubria subsigillata	0010020000222000100202112002110000020000102000221110100001111010211000010011111102
Bufo granulosus	0010001110200120100212101002110000011000101001310000001001120000202000011111110000
Bufo variegatus	0101000100100100100110001002110000011000001001310000001001120000202000011111110000
Ceratophrys cranwelli	0010021110222120100202122000121000010000111020010001001001130000201000010011110002
Conraua crassipes	0101020000111100000202112002110000020001102000220011100011120000202000010011110000
Cardioglossa cyaneospila	0101020100110101010112101013010000021001002000210021100010100001100000110011110011
Cardioglossa leucomystax	0001020100110110010112101013010000021001002001210021100010100001100000110011110011
Chacophrys pierottii	0010021110222120100202122000121020010000211001010001101001130000201000010011110000
Chiromantis rufescens	1101020000111100000212101022110000021001002000220021101111011400203140010011110000
Flectonotus fitzgeraldi	0101000000111100010211101001110000011001001001010000000101111100201110010000??001
Amnirana albolabris	1101010000111100000212101021110000020000002000120011100001120300201020010011110000
Hyla andina	0001000100111100010212101001110000011001001001010001000101121100203110010011110000
Hymenochirus boettgeri	0000021010010122011?00000???1????10110001?013100201000211000003200000000100000
Hyperolius castaneus	0101110100111100000112101021000000021001002001210021000111111210101121001111001
Hyperolius kivuensis	0101110100111100000112101021000000021001002001210021000111111210101121010011110000
Hyla nana	0001000100101101000112101001110000011001001001010001000101121100203110010011110001
Hoplobatrachus occipitalis	0000020010211000110212112002110000020001102001220011000011121010201001010011110002
Hyla rivularis	0000000000111100010211101001110000011000001002310000000101131100201110010011110000
Kassina senegalensis	0001120100111100000112101031000000021000002001210021000111111211101121110011110000
Leptodactylus bufonius	0001020100111100010202101001110000011001101001020000100011121001212001110011110000
Leptodactylus latinasus	0001020000111101010202101001110000011001101001020000000011120011212001110011110000
Leptodactylus chaquensis	0001020000211100110202101001110000011000101001020000100001121110202111010011110002
Leptopelis christyi	1101021000111100000202101011010000021001002000110021101111111100101110010011110000
Lepidobatrachus laevis	0010021110222120100202122100121020010000111011010001001001130000201000010010100002
Lepidobatrachus llanensis	0010021110222120100202122100121020010000111011010001001001130000201000010011010002
Melanophryniscus rubriventris	0000021110100100100110001003110000011000001000010010001011120000201000010011110000
Odontophrynus americanus	0000021100201110100212101011110000011000101001310001001011130000201000010011110000
Pyxicephalus adspersus	0010021010222000100202112002110000020000102001220011101001130010201000010011110002
Prhynomantis bifasciatus	1101100100000100000112001001010000021001002000311230000101020400201040010013000000
Physalaemus biligonigerus	0001010100101100000202101013110000011000001001020001000001130000201000010011110000
Pleurodema bufonina	0001010100111100000210101012110000011000001001020001001011120000201000010011110000
Pseudis paradoxus	0001020100121101000202101002110000011000101001010000000111110000201001010011110000
Phyllomedusa lemur	0101001000211100000101101007?100000110000010003100001001011211002011100110111001
Phyllomedusa sauvagii	0101001000211100100202101000110000011000101001010001001101121100201110011011110002
Phlyctimantis verrucosus	0101011000111110000021210102200000002100100200021002001111111210101121010011110000
Opisthothylax immaculatus	0101110000111100000112101021000000021001002000210021001101111100101110010011110000
Afrana angolensis	1101010010111100000212101001110000020000102000120010100001121110201000010011110002
Rhiderma darwinii	0101100000110101000111001001110000010001001001010010000001100000200000010011110001
Spea bombifrons	0101001000111101100200001103110000010100110001010000001000130000001000010011110000
Scaphiopus couchii	0010021110221100110200001103110000010100110001010000001000130000001000010011110000
Scinax fuscovarius	0001010000111100000212101001110000011001001001010000001101121200202120010011110001
Xenopus laevis	1000020000212102001O?000000??1000000110011010101001001000111110000000000001000000

Journal compilation © 2006 Blackwell Verlag, Berlin, JZS **44**(2), 153–166 (2006)

Appendix 3. Continued

Phrynobatrachus versicolor	0101010000111101000112101003110100021001002000120021100011120200201020010011111000
Phrynobatrachus dendrobates	1101020000111101000112101003110100021001002001120021100011120200201020010011111000
Phrynobatrachus petropedetoides	0101020100111101000112101003110100021001002001120021100011120200201020010011111001
Phrynobatrachus acutirostris	0101020000111101000112101003110100021001002000120020100011110200201020010011111000
Phrynobatrachus sulfureogularis	0101010100111101000112101003110100021001002001220021100000111020020102001001111000
Ptychadena uzungwensis	1101020000111110000021200100111000000?101000200122012012010000011211110203111010011111000
Ptychadena mascareniensis	1101020000111110000021200100111000000?101000200122012010000011211110203111010011111000
Ptychadena christyi	1101020000111110000021200100111000000?101000200122012010000011211110203111010011111000
Ptychadena chrysogaster	1101020000111110000021200100111000000?101000200122012010000011211110203111010011111000
Schoutedenella pyrrhoscelis	0001010100000111010112101013010000011001002001211021100011100201120020110000??2011
Schoutedenella sylvatica	0001010100000111010112101013010000011001002001211021100011100201120020110000??2011
Schoutedenella schubotzi	0001010100000111010112101013010000011001002001211021100011100201120020110000??2011
Schoutedenella lameerei	0001010100000111010112101013010000011001002001211021100011100201120020110000??2011